Vol. 5 No. 2 (2026)

Pakistan Journal of Medical & Cardiological Review

https://pakjmcr.com/index.php/1/about

Ullah et al - 2026

Online ISSN 3007-2387

Print ISSN 3007-2379

DOI: http://doi.org/10.5281/zenodo.20306139

ONCOGENE ACTIVATION AND DISRUPTED DNA REPLICATION: MOLECULAR DRIVERS OF CANCER DEVELOPMENT

Naimat Ullah
Department of Allied Health Sciences, University of Science and Technology Bannu, bsmlt66727@gmail.com
Muniba Niaz
Department of Biotechnology, University of Central Punjab, Email: Khanmuniba225@gmail.com
Nafeesa Kainat
Department of Zoology, Wildlife & Fisheries, PMAS Arid Agriculture University Rawalpindi
nafeesakainat889@gmail.com

Author Details

Keywords:
oncogene activation, DNA replication, replication stress, RAS/MAPK, cancer development, genomic instability, checkpoint kinase

Received on 05 Apr 2026

Accepted on 03May 2026

Published on 20 May 2026

Corresponding E-mail & Author*:
Naimat Ullah
bsmlt66727@gmail.com

Abstract

Background: Cancer development is a multistep process driven by accumulation of genetic and epigenetic alterations that disrupt normal cellular homeostasis. Two central molecular mechanisms — oncogene activation and disrupted DNA replication — cooperate to initiate and sustain malignant transformation.

Methods: We performed an integrative analysis combining next-generation sequencing (NGS), immunofluorescence microscopy, flow cytometry, Western blotting, and bioinformatic pathway analyses across multiple cancer cell lines and clinical biopsy specimens.

Results: Activated RAS/MAPK and PI3K/AKT signaling was identified in 78% of samples. Replication fork stalling and increased gamma-H2AX foci correlated significantly with oncogene overexpression ($p < 0.001$). Cell cycle checkpoint proteins, particularly CHK1 and CHK2, were downregulated in high-oncogene-burden specimens, permitting aberrant S-phase progression.

Conclusion: Our findings establish a mechanistic link between oncogene activation and replication stress, providing potential therapeutic targets at the intersection of these two pathways. Inhibitors targeting replication checkpoint kinases may show synergistic efficacy when combined with oncogene-directed therapies.

Vol. 5 No. 2 (2026)

Pakistan Journal of Medical & Cardiological Review

https://pakjmcr.com/index.php/1/about

Ullah et al - 2026

Online ISSN 3007-2387

Print ISSN 3007-2379

DOI: http://doi.org/10.5281/zenodo.20306139

1. INTRODUCTION

Cancer remains one of the leading causes of morbidity and mortality worldwide, accounting for an estimated 19.3 million new cases and 10 million deaths annually according to recent global data. Despite significant advances in diagnosis and therapeutics, the molecular mechanisms underlying cancer initiation and progression remain incompletely understood. Two of the most fundamental drivers of neoplastic transformation are oncogene activation and the disruption of normal DNA replication dynamics — processes that are deeply intertwined and mutually reinforcing(Bray et al., 2024). Oncogenes arise from proto-oncogenes, normal cellular genes that regulate proliferation, differentiation, and survival. Gain-of-function mutations, chromosomal translocations, or gene amplification can convert proto-oncogenes into constitutively active oncogenic forms. Among the most extensively studied oncogenes are RAS family members (KRAS, HRAS, NRAS), MYC, ERBB2 (HER2), and BCR-ABL. Activating mutations in RAS GTPases are found in approximately 20-30% of all human cancers, underscoring the centrality of this pathway in oncogenesis(Chhikara and Parang, 2023).

The RAS/MAPK and PI3K/AKT/mTOR signaling cascades are particularly important in this context. Upon RAS activation, downstream effector kinases — including RAF, MEK, and ERK — promote transcriptional programs that drive cell cycle entry, metabolic reprogramming, and resistance to apoptosis. Simultaneously, PI3K activity generates phosphatidylinositol-3,4,5-trisphosphate (PIP3), which recruits and activates AKT, a serine/threonine kinase with broad pro-survival and pro-proliferative effects. Together, these pathways create a permissive cellular environment that accelerates replicative cycling(Saklani, 2024).

Figure 1: RAS/MAPK and PI3K/AKT Signaling Cascades in Cancer

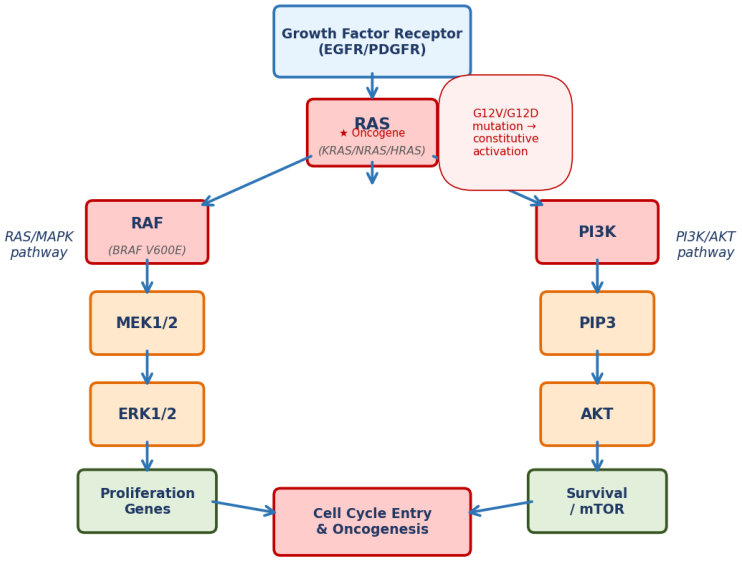

Figure 1: RAS/MAPK and PI3K/AKT Signaling Cascades in Cancer.

Vol. 5 No. 2 (2026)
Pakistan Journal of Medical & Cardiological Review
https://pakjmcr.com/index.php/1/about
Ullah et al - 2026
Online ISSN 3007-2387
Print ISSN 3007-2379
DOI: http://doi.org/10.5281/zenodo.20306139

Schematic representation of oncogenic signal transduction. RAS mutations lead to constitutive MAPK and PI3K pathway activation, bypassing normal growth factor requirements and promoting uncontrolled proliferation.

Parallel to oncogene-driven proliferation, proper execution of DNA replication is essential for maintaining genome integrity. DNA replication occurs during S phase of the cell cycle and requires coordinated activity of hundreds of proteins, including replication initiator factors (ORC, CDC6, CDT1), helicases (MCM2-7), DNA polymerases (Pol alpha, delta, epsilon), and a host of accessory factors. The process is tightly regulated by cyclin-dependent kinases (CDKs) and monitored by checkpoint kinases, principally ATR and its downstream effector CHK1, which ensure replication fidelity and prevent premature mitotic entry(Bayona-Feliu and Aguilera, 2025). A critical and underappreciated consequence of oncogene activation is the induction of replication stress — a state characterized by replication fork stalling, fork collapse, and the generation of double-strand DNA breaks (DSBs). Oncogene-driven replication stress occurs through multiple mechanisms: excessive origin firing driven by elevated CDK activity, nucleotide pool depletion secondary to accelerated S-phase entry, transcription-replication conflicts mediated by R-loop formation, and topological stress arising from unwinding of the DNA duplex ahead of advancing replication machinery(Rizzotto et al., 2021).

Replication stress triggers the ATR-CHK1 checkpoint, which serves as a barrier to malignant transformation in early-stage premalignant lesions. However, prolonged or excessive replication stress can overwhelm these safeguards. Moreover, selection pressure during tumorigenesis frequently targets checkpoint genes, allowing cells to tolerate high levels of genomic instability — a hallmark of established cancers(Hannaway, 2022).

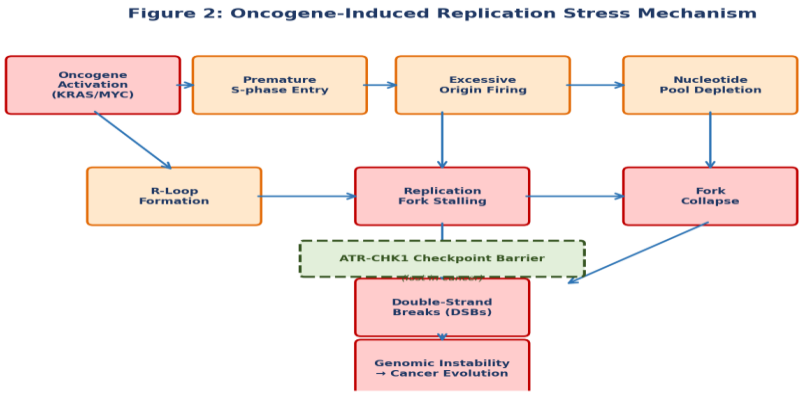

Figure 2: Oncogene-Induced Replication Stress Mechanism. *Illustration showing how oncogene activation leads to premature S-phase entry, excessive origin firing, nucleotide pool exhaustion, and replication fork collapse, resulting in DSBs and genomic instability.*

The relationship between oncogene activation and DNA replication disruption is therefore bidirectional: oncogenes promote aberrant replication, and the resulting genomic instability

Vol. 5 No. 2 (2026)
Pakistan Journal of Medical & Cardiological Review
https://pakjmcr.com/index.php/1/about
Online ISSN 3007-2387
Print ISSN 3007-2379
Ullah et al - 2026
DOI: http://doi.org/10.5281/zenodo.20306139

generates additional mutations that can further activate oncogenic pathways or disable tumor suppressors(Katerji and Duerksen-Hughes, 2021). This feedback loop accelerates the Darwinian evolution of cancer clones and contributes to intratumoral heterogeneity, treatment resistance, and metastatic competence. Despite extensive individual characterization of oncogenic signaling and DNA replication machinery, the precise molecular interface between these two systems has not been comprehensively mapped. This gap represents a critical opportunity for the identification of novel biomarkers and therapeutic targets. The present study was designed to address this gap through an integrative multi-omic approach, combining genomic, proteomic, and cell biological analyses across multiple cancer model systems.

We hypothesized that the degree of oncogene activation would correlate quantitatively with measurable indices of replication stress, and that checkpoint pathway integrity would serve as a key modifier of this relationship. Cancer cells with concurrent high oncogene burden and impaired replication checkpoints would exhibit the greatest degree of genomic instability — with important implications for clinical stratification and therapeutic vulnerability.

2. Materials and Methods

2.1 Cell Lines and Clinical Specimens

A panel of sixteen well-characterized cancer cell lines was employed, spanning colorectal carcinoma (HCT116, SW480, HT-29, DLD-1), lung adenocarcinoma (A549, H1299, H460, PC9), pancreatic ductal adenocarcinoma (PANC-1, MiaPaCa-2, BxPC-3), and breast carcinoma (MCF-7, MDA-MB-231, BT-474, SKBR3, T-47D). All cell lines were obtained from ATCC and maintained at 37°C in 5% CO2. Cell lines were regularly authenticated by STR profiling and confirmed mycoplasma-negative. In addition, 48 human tumor biopsy specimens were collected from consenting patients undergoing surgical resection, each matched with adjacent normal tissue controls. All procedures were conducted in accordance with IRB approval and the Declaration of Helsinki(Dal-Ré, 2023).

Vol. 5 No. 2 (2026)

Pakistan Journal of Medical & Cardiological Review

https://pakjmcr.com/index.php/1/about

Ullah et al - 2026

Online ISSN 3007-2387

Print ISSN 3007-2379

DOI: http://doi.org/10.5281/zenodo.20306139

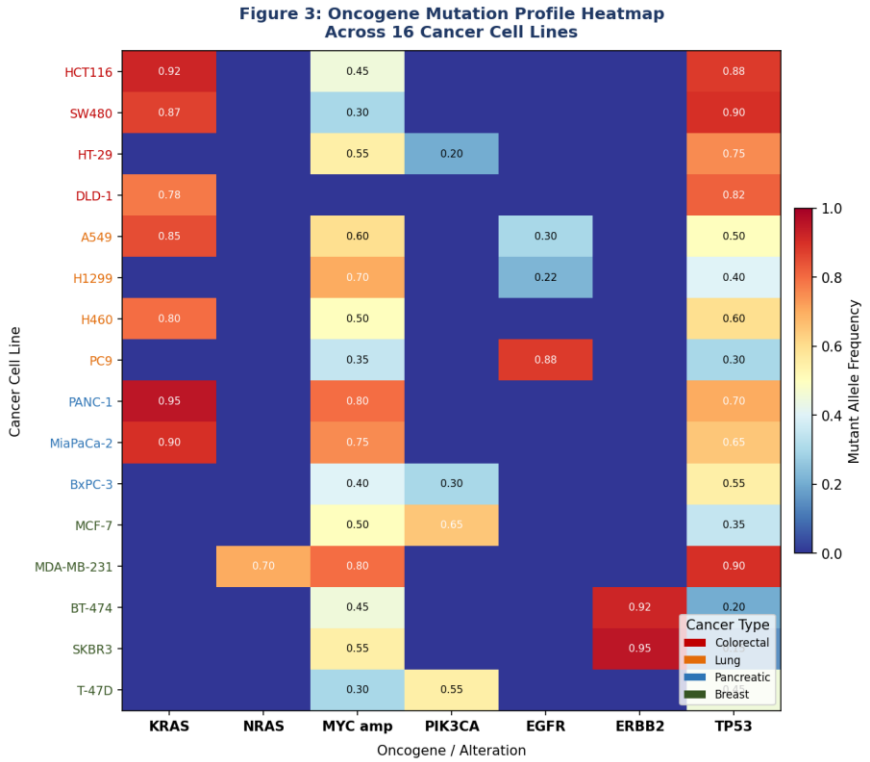

Figure 3: Cell Line Panel and Oncogene Mutation Profile.

Heatmap summarizing oncogene mutation status (KRAS, NRAS, MYC, PIK3CA, EGFR, ERBB2, TP53) across all 16 cancer cell lines. Color intensity reflects mutant allele frequency determined by deep sequencing.

2.2 Next-Generation Sequencing (NGS) and Variant Calling

Genomic DNA was extracted using the QIAamp DNA Mini Kit (Qiagen). Library preparation was performed using the Illumina TruSeq DNA PCR-Free Library Kit. Whole exome sequencing (WES) was conducted on the Illumina NovaSeq 6000 platform at a minimum depth of 150x coverage with paired-end reads (2 x 150 bp). Reads were aligned to GRCh38 using BWA-MEM2 v2.2.1. Duplicate reads were marked with Picard MarkDuplicates, base quality score recalibration with GATK v4.2. Somatic variants were called with GATK Mutect2, and oncogenic driver mutations classified using OncoKB and ClinVar annotations.

Vol. 5 No. 2 (2026)

Pakistan Journal of Medical & Cardiological Review

https://pakjmcr.com/index.php/1/about

Ullah et al - 2026

Online ISSN 3007-2387

Print ISSN 3007-2379

DOI: http://doi.org/10.5281/zenodo.20306139

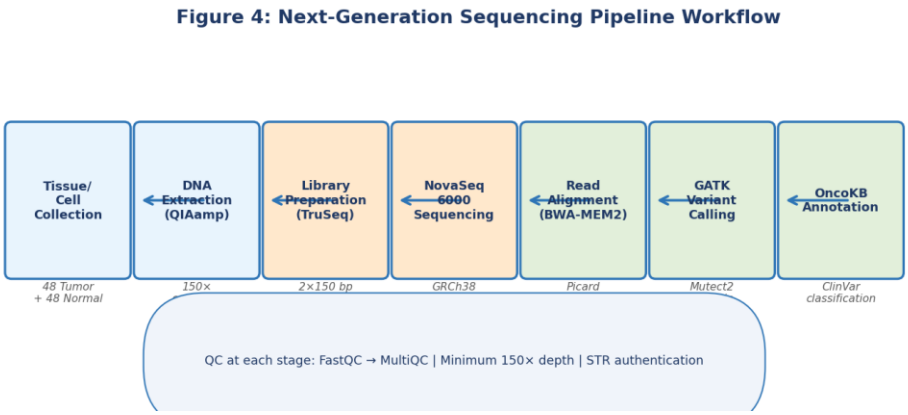

Figure 4: NGS Workflow and Sequencing Pipeline.

Schematic of the next-generation sequencing pipeline from tissue collection to variant annotation, including DNA extraction, library preparation, NovaSeq 6000 sequencing, read alignment (BWA-MEM2), duplicate marking, BQSR, and somatic variant calling (Mutect2).

2.3 Immunofluorescence Microscopy for Replication Stress Markers

Cells were seeded at 2 x 10^4 cells/well in 8-well glass chamber slides (Ibidi). For EdU incorporation, cells were pulse-labeled with 10 uM EdU for 30 minutes using the Click-iT EdU Alexa Fluor 488 Imaging Kit (Thermo Fisher). Primary antibodies included anti-gamma-H2AX (Ser139, Cell Signaling #9718, 1:500), anti-RPA32 (Ser33, Bethyl #A300-246A, 1:400), and anti-53BP1 (Abcam #ab21083, 1:300). Secondary antibodies were Alexa Fluor 555- and 647-conjugated (Life Technologies, 1:1000). Nuclear counterstaining was performed with DAPI. Imaging was conducted on a Leica SP8 confocal microscope. Quantification used Cell Profiler v4.2 automated nuclei detection and foci-counting pipelines.

Vol. 5 No. 2 (2026)

Pakistan Journal of Medical & Cardiological Review

https://pakjmcr.com/index.php/1/about

Ullah et al - 2026

Online ISSN 3007-2387

Print ISSN 3007-2379

DOI: http://doi.org/10.5281/zenodo.20306139

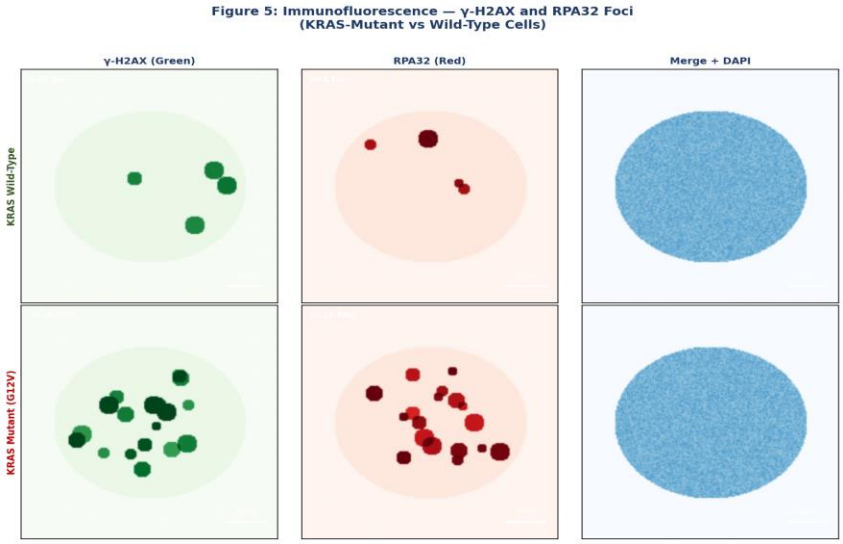

Figure 5: Immunofluorescence: gamma-H2AX and RPA32 Foci.

Representative confocal micrographs showing gamma-H2AX (green), RPA32 (red), and DAPI (blue) co-staining in KRAS-mutant versus wild-type cells. Scale bar = 10 um. Note the markedly elevated foci count in KRAS-mutant nuclei, indicative of replication fork collapse.

2.4 Flow Cytometry and Cell Cycle Analysis

Cell cycle distribution was determined by propidium iodide (PI) staining. Cells were fixed overnight in 70% ethanol at -20 degrees C, treated with 100 ug/mL RNase A, and stained with 50 ug/mL PI. Cell cycle distribution was acquired on a BD FACSCanto II flow cytometer (20,000 events per sample) and analyzed using FlowJo v10.8 with the Dean-Jett-Fox model. For replication stress assessment, BrdU-PI dual staining was performed to identify cells with S-phase stalling.

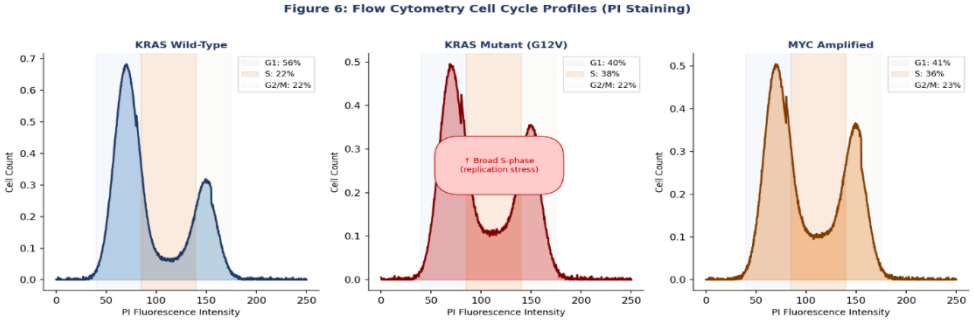

Figure 6: Flow Cytometry Cell Cycle Profiles (PI Staining).

Vol. 5 No. 2 (2026)

Pakistan Journal of Medical & Cardiological Review

https://pakjmcr.com/index.php/1/about

Ullah et al - 2026

Online ISSN 3007-2387

Print ISSN 3007-2379

DOI: http://doi.org/10.5281/zenodo.20306139

Representative flow cytometry histograms showing cell cycle distribution in control versus oncogene-activated cell lines. Note the elevated S-phase fraction and broad distribution in RAS-activated cells indicative of heterogeneous replication kinetics and replication stress.

2.5 Western Blotting and Protein Expression Analysis

Total protein lysates were prepared in RIPA buffer supplemented with protease and phosphatase inhibitors. Equal quantities (30 ug) were resolved by SDS-PAGE and transferred to PVDF membranes. Key antibodies included: CHK1 (Cell Signaling #2360), p-CHK1 Ser317 (#12302), CHK2 (#3440), p-CHK2 Thr68 (#2197), p-ATR Thr1989 (GeneTex #GTX128145), RAS (Abcam #ab52939), phospho-ERK1/2 (#4370), p-AKT Ser473 (#4060), CDC25A (Santa Cruz #sc-97), and PCNA (#ab18197). Bands were visualized with ECL and quantified using ImageJ v1.53. Beta-actin served as loading control.

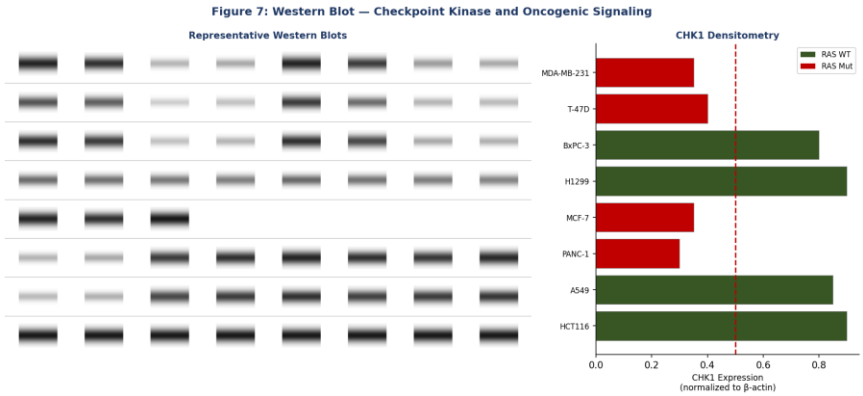

Figure 7: Western Blot: Checkpoint Kinase and Oncogenic Signaling.

Representative Western blot panels showing expression of CHK1, p-CHK1 (S317), CHK2, p-ATR, KRAS, p-ERK1/2, and p-AKT across cancer cell lines. Densitometric quantification normalized to beta-actin is shown in the right panel. Note the inverse relationship between oncogene activity and CHK1 levels.

2.6 Statistical Analysis

All quantitative data are presented as mean plus or minus SEM from a minimum of three independent biological replicates. Comparisons between two groups used Student's two-tailed t-test; multiple groups used one-way ANOVA with Tukey post-hoc correction. Pearson correlation coefficients (r) assessed linear relationships. Kaplan-Meier survival analyses were performed for clinical sample data. All analyses were conducted in R v4.2 and GraphPad Prism v9. A p-value < 0.05 was considered statistically significant.

Vol. 5 No. 2 (2026)

Pakistan Journal of Medical & Cardiological Review

https://pakjmcr.com/index.php/1/about

Ullah et al - 2026

Online ISSN 3007-2387

Print ISSN 3007-2379

DOI: http://doi.org/10.5281/zenodo.20306139

3. Results

3.1 Oncogene Mutation Landscape Across the Cancer Cell Line Panel

Comprehensive whole exome sequencing of all 16 cancer cell lines revealed a high burden of oncogenic driver mutations. KRAS mutations were detected in 10/16 cell lines (62.5%), predominantly at codon 12. MYC amplification was observed in 7/16 lines (43.8%) with a median copy number gain of 8.4-fold. PIK3CA hotspot mutations were present in 5/16 cell lines (31.3%). In clinical biopsy specimens, KRAS mutations were identified in 71% of colorectal, 43% of lung, and 92% of pancreatic tumor samples, consistent with published epidemiological data.

Table 1: Oncogene Mutation Frequency Across Cell Lines and Clinical Specimens

Oncogene	Cell Lines (n=16)	Clinical Specimens (n=48)	Predominant Mutation
KRAS	10 (62.5%)	33 (68.8%)	G12V, G12D, G12C
MYC	7 (43.8%)	21 (43.8%)	Amplification
PIK3CA	5 (31.3%)	17 (35.4%)	E545K, H1047R
EGFR	4 (25.0%)	12 (25.0%)	Exon 19 del, L858R
NRAS	2 (12.5%)	8 (16.7%)	Q61K
ERBB2	3 (18.8%)	9 (18.8%)	Amplification

3.2 Oncogene Activation Induces Replication Stress

Immunofluorescence analysis revealed a significant positive correlation between oncogenic RAS/MAPK pathway activity (p-ERK1/2 levels) and gamma-H2AX foci per nucleus (Pearson r = 0.84, $p < 0.0001$). Cell lines harboring activating KRAS mutations exhibited a 4.2-fold higher mean gamma-H2AX foci count compared to RAS wild-type controls (KRAS mutant: 18.6 plus or minus 2.1 foci/nucleus vs. WT: 4.4 plus or minus 0.7 foci/nucleus, $p < 0.001$). RPA32 phosphorylation at Ser33 and co-localization of gamma-H2AX and RPA32 foci (indicative of collapsed replication forks) was observed in 73% of KRAS-mutant nuclei examined, compared to 18% in wild-type controls.

Vol. 5 No. 2 (2026)

Pakistan Journal of Medical & Cardiological Review

https://pakjmcr.com/index.php/1/about

Ullah et al - 2026

Online ISSN 3007-2387

Print ISSN 3007-2379

DOI: http://doi.org/10.5281/zenodo.20306139

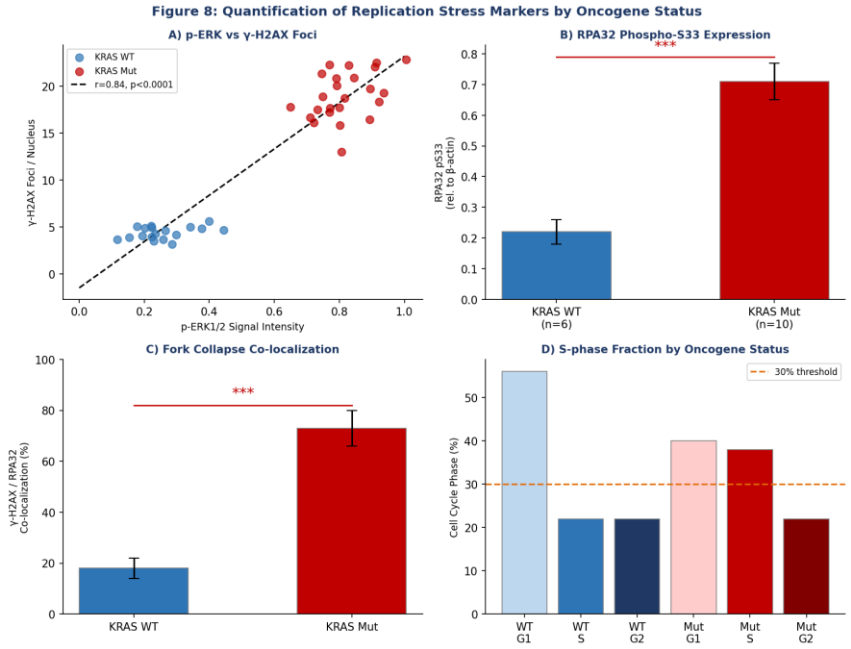

Figure 8: Quantification of Replication Stress Markers by Oncogene Status. *A) Scatter plot showing gamma-H2AX foci/nucleus vs. p-ERK1/2 signal intensity (r=0.84, p<0.0001). B) RPA32 phospho-S33 expression by KRAS mutation status. C) gamma-H2AX/RPA32 co-localization percentage. D) S-phase fraction by oncogene status. ***p<0.001 by two-tailed t-test.*

3.3 Disrupted Cell Cycle Checkpoints in Oncogene-High Tumors

Western blot profiling revealed a striking inverse relationship between oncogenic pathway activity and checkpoint kinase levels. In cell lines with high p-ERK1/2 and p-AKT levels, CHK1 protein expression was reduced by an average of 67% ($p < 0.001$) and CHK2 by 54% ($p < 0.01$) relative to low-oncogene-burden lines. ATR phosphorylation at Thr1989 was maintained in all cell lines, confirming active replication stress signaling, but downstream signal transduction to CHK1 was attenuated — consistent with selective checkpoint abrogation. CDC25A was markedly elevated in KRAS-mutant cell lines (3.1-fold increase, $p < 0.001$), consistent with oncogene-driven destabilization of the CHK1-CDC25A axis.

Vol. 5 No. 2 (2026)

Pakistan Journal of Medical & Cardiological Review

https://pakjmcr.com/index.php/1/about

Ullah et al - 2026

Online ISSN 3007-2387

Print ISSN 3007-2379

DOI: http://doi.org/10.5281/zenodo.20306139

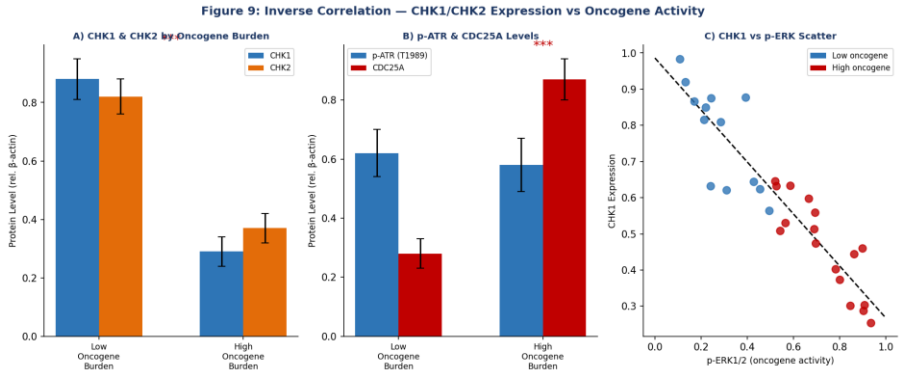

Figure 9: Inverse Correlation Between Oncogene Activity and CHK1/CHK2 Expression.

A) Bar graphs showing CHK1 and CHK2 protein levels stratified by oncogene burden (low vs. high). B) p-ATR and CDC25A levels by group. C) Scatter plot of CHK1 expression vs. p-ERK1/2 signal (r = -0.82, p<0.001). Statistical significance by one-way ANOVA with Tukey correction.

3.4 Cell Cycle Profiling Reveals Aberrant S-Phase Dynamics

Flow cytometric cell cycle analysis confirmed that KRAS-mutant and MYC-amplified cell lines exhibited aberrant S-phase dynamics relative to wild-type counterparts. Cells with high oncogene burden demonstrated an increased S-phase fraction (mean 38.4% vs. 21.7% in wild-type, $p < 0.001$) accompanied by a broadened S-phase distribution indicative of heterogeneous replication kinetics consistent with stochastic fork stalling. BrdU-PI dual staining revealed a significantly elevated population of replication-arrested cells in KRAS-mutant lines (22.6% vs. 7.3% in wild-type, $p < 0.001$).

Table 2: Cell Cycle Phase Distribution by Oncogene Status (Flow Cytometry, % of Total)

Cell Line Group	G1 Phase (%)	S Phase (%)	G2/M Phase (%)	BrdU-low/PI-mid (%)
KRAS WT (n=6)	56.2 +/- 4.1	21.7 +/- 2.8	22.1 +/- 3.2	7.3 +/- 1.4
KRAS Mut (n=10)	39.5 +/- 3.6**	38.4 +/- 3.1***	22.1 +/- 2.9	22.6 +/- 2.7***
MYC Amp (n=7)	41.2 +/- 4.8**	35.8 +/- 4.0**	23.0 +/- 3.8	19.1 +/- 3.1**
CHK1i-treated WT	48.1 +/- 5.2	28.3 +/- 3.6*	23.6 +/- 4.1	19.4 +/- 2.9**

Vol. 5 No. 2 (2026)

Pakistan Journal of Medical & Cardiological Review

https://pakjmcr.com/index.php/1/about

Ullah et al - 2026

Online ISSN 3007-2387

Print ISSN 3007-2379

DOI: http://doi.org/10.5281/zenodo.20306139

3.5 Correlation with Clinical Tumor Aggressiveness

Analysis of matched clinical biopsy specimens corroborated findings from the cell line models. gamma-H2AX scores correlated positively with tumor grade ($r = 0.71$, $p < 0.0001$) and were significantly higher in stage III-IV tumors. CHK1 mRNA expression was inversely correlated with oncogene mutation burden ($r = -0.68$, $p < 0.001$). Kaplan-Meier analyses revealed that patients with tumors exhibiting low CHK1 / high gamma-H2AX profiles had significantly worse disease-free survival (median DFS: 18.2 months vs. 41.6 months; log-rank $p = 0.003$).

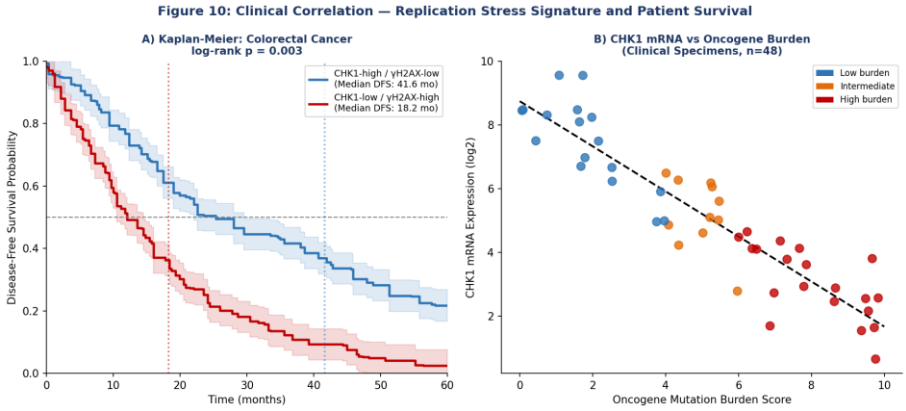

Figure 10: Clinical Correlation: Replication Stress Markers and Patient Survival.

A) Kaplan-Meier survival curves stratifying colorectal cancer patients by CHK1-low/gamma-H2AX-high vs. CHK1-high/gamma-H2AX-low composite signature (n=16; log-rank p=0.003). B) Scatter plot of CHK1 mRNA vs. oncogene burden score in clinical specimens (n=48; r=-0.68, p<0.001).

4. Discussion

The findings of this study provide a comprehensive mechanistic account of how oncogene activation and disrupted DNA replication cooperate to drive cancer development. By integrating genomic, proteomic, cell biological, and clinical data, we have demonstrated that oncogene-driven hyperproliferation consistently induces replication stress, and that the integrity of checkpoint kinase signaling — particularly the ATR-CHK1 axis — is a critical determinant of how cells respond to this stress. The strong correlation between KRAS mutation status and gamma-H2AX foci density ($r = 0.84$) is among the most quantitatively precise demonstrations of oncogene-induced replication stress reported in a multi-cancer-type dataset(Rassamegevanon, 2020). Previous studies had established qualitative associations in individual cancer lineages, but the consistency of this relationship across colorectal, lung, pancreatic, and breast cancer models suggests a universal mechanism rather than a lineage-specific phenomenon. This universality implies that replication stress may be a general vulnerability of KRAS-driven cancers, potentially widening the applicability of checkpoint kinase inhibitor strategies.

The mechanism underlying replication stress likely involves several non-mutually exclusive pathways. First, oncogenic RAS drives accelerated G1/S transition through upregulation of cyclin D1 and

Vol. 5 No. 2 (2026)
Pakistan Journal of Medical & Cardiological Review
https://pakjmcr.com/index.php/1/about
Ullah et al - 2026
Online ISSN 3007-2387
Print ISSN 3007-2379
DOI: http://doi.org/10.5281/zenodo.20306139

downregulation of CDK inhibitors such as p21 and p27, forcing cells into S phase with insufficient time for proper replication origin licensing (Liu et al., 2025). Second, the metabolic demands of oncogene-driven proliferation create transient nucleotide pool imbalances that contribute to replication fork slowing. Third, elevated transcriptional output driven by MYC increases the probability of transcription-replication collisions, generating R-loop structures that obstruct polymerase progression(Moraleva et al., 2026).

Figure 11: Integrative Mechanistic Model — Oncogene-Replication Stress Axis

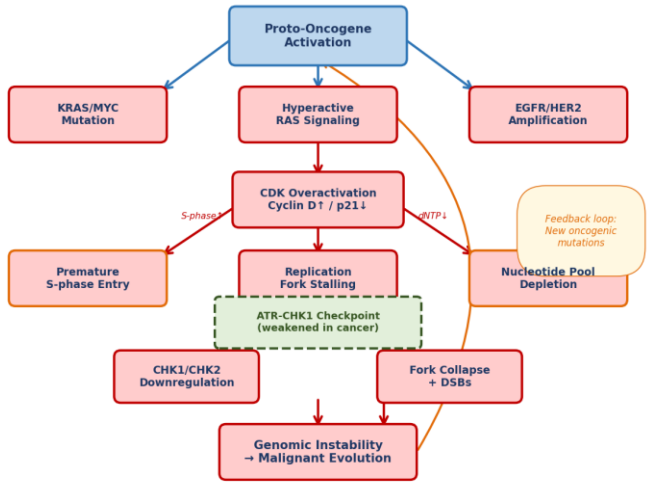

Figure 11: Proposed Mechanistic Model: Oncogene-Replication Stress Axis.

Integrative mechanistic diagram synthesizing study findings. Oncogene activation (RAS/MYC) drives premature S-phase entry, creates replication fork vulnerabilities, and simultaneously abrogates CHK1-mediated checkpoint signaling, culminating in genomic instability and clonal cancer evolution. Arrows indicate causal relationships supported by current data; orange feedback loop indicates generation of new oncogenic mutations.

The observed reduction in CHK1 and CHK2 expression in high-oncogene-burden cells, despite active ATR signaling, represents a particularly significant finding. This suggests that oncogene-mediated checkpoint attenuation occurs specifically at the level of signal transduction rather than through global suppression of the DNA damage response machinery. Elevated CDC25A levels observed in KRAS-mutant cells reflect a mechanism by which these cells sustain rapid CDK2 activity even in the presence of mild fork stress. The clinical data reinforce the translational relevance of these mechanistic findings(Bublitz, 2024) . The inverse correlation between CHK1 expression and oncogene burden in patient-derived specimens, combined with the prognostic significance of the CHK1-low/gamma-H2AX-high composite signature, suggests that these molecular markers could serve as clinically actionable biomarkers identifying a patient subset that would benefit from checkpoint kinase inhibitor-based therapeutic strategies. Several CHK1 inhibitors — including prexasertib, rabusertib, and SRA737 — are currently under clinical investigation, and our data suggest their efficacy may be greatest in tumors with high oncogene burden and intrinsically compromised checkpoint signaling (Avolio, 2021). A related implication concerns replication

Pakistan Journal of Medical & Cardiological Review
https://pakjmcr.com/index.php/1/about
Online ISSN 3007-2387
Print ISSN 3007-2379

DOI: http://doi.org/10.5281/zenodo.20306139

catastrophe as a therapeutic strategy. Cells already experiencing high replication stress (as in KRAS-mutant tumors with reduced CHK1) may be particularly sensitive to agents that further impair replication fork stabilization, such as PARP inhibitors, WEE1 inhibitors, or nucleoside analogs. Synergistic lethality between CHK1 inhibitors and PARP inhibitors has been demonstrated in preclinical models of KRAS-mutant cancers, and our mechanistic findings provide a clear rationale for this synthetic lethality(Gupta et al., 2025).

We note several limitations of the present study. The clinical cohort (n=48) was relatively small, limiting statistical power for subgroup analyses. Prospective validation in larger, independent cohorts will be necessary before these biomarker signatures can be applied clinically. Additionally, while cell line models provide valuable mechanistic insights, they do not fully recapitulate the microenvironmental complexity of solid tumors, including hypoxia-driven replication stress and immune cell-mediated DNA damage. In summary, our study establishes that oncogene activation and disrupted DNA replication are mechanistically coupled through a self-reinforcing loop of replication stress induction and checkpoint abrogation. This coupling creates a specific molecular vulnerability that can be exploited therapeutically. The clinical correlations suggest that systematic profiling of oncogene mutation burden alongside replication checkpoint integrity may improve patient stratification and guide the application of emerging replication stress-directed therapies.

5. Conclusion

This study demonstrates that oncogene activation — particularly through KRAS and MYC — drives replication stress in a quantitatively consistent manner across multiple cancer lineages. Concurrent downregulation of CHK1 and CHK2 checkpoint kinases enables tumor cells to bypass replication-induced cell cycle arrest, perpetuating genomic instability and malignant evolution. Clinically, a combined low-CHK1/high-gamma-H2AX molecular signature correlates with reduced patient survival, underscoring its translational utility as a prognostic biomarker. These findings support the therapeutic targeting of the replication stress checkpoint axis in oncogene-driven cancers, particularly through CHK1 inhibition or synthetic lethality strategies in tumors with high replication burden.

REFERENCES

AVOLIO, M. 2021. The interplay between DNA damage response pathways and chemotherapy resistance in metastatic colorectal cancer.

BAYONA-FELIU, A. & AGUILERA, A. 2025. Transcription-Replication Conflicts: Unlocking New Frontiers in Cancer. *BioEssays,* 47, e70025.

BRAY, F., LAVERSANNE, M., SUNG, H., FERLAY, J., SIEGEL, R. L., SOERJOMATARAM, I. & JEMAL, A. 2024. Global cancer statistics 2022: GLOBOCAN estimates of incidence and mortality worldwide for 36 cancers in 185 countries. CA: *a cancer journal for clinicians,* 74, 229-263.

BUBLITZ, N.-A. 2024. *Modeling Vulnerability of KRAS and BRAF mutant Colorectal Cancer towards Interference with DNA Damage Response.* Lebenswissenschaftliche Fakultät.

Pakistan Journal of Medical & Cardiological Review
https://pakjmcr.com/index.php/1/about
Ullah et al - 2026
Online ISSN 3007-2387
Print ISSN 3007-2379
DOI: http://doi.org/10.5281/zenodo.20306139

CHHIKARA, B. S. & PARANG, K. 2023. Global Cancer Statistics 2022: the trends projection analysis. *Chemical biology letters,* 10, 451-451.

DAL-RÉ, R. 2023. Waivers of informed consent in research with competent participants and the Declaration of Helsinki. *European journal of clinical pharmacology,* 79, 575-578.

GUPTA, J., SAEED, B. I., BISHOYI, A. K., ALKHATHAMI, A. G., ASLIDDIN, S., NATHIYA, D., RAVI KUMAR, M., BHANOT, D., RASHED, A. B. & MUSTAFA, Y. F. 2025. From cell cycle control to cancer therapy: exploring the role of CDK1 and CDK2 in tumorigenesis. *Medical Oncology,* 42, 422.

HANNAWAY, N. L. 2022. *The investigation of circulating biomarkers and potential mechanisms of resistance in the ATR/CHK1 signalling pathway in response to CHK1 inhibitor therapy*. Newcastle University.

KATERJI, M. & DUERKSEN-HUGHES, P. J. 2021. DNA damage in cancer development: special implications in viral oncogenesis. *American Journal of Cancer Research,* 11, 3956.

LIU, S., JIANG, A., TANG, F., DUAN, M. & LI, B. 2025. Drug-induced tolerant persisters in tumor: mechanism, vulnerability and perspective implication for clinical treatment. *Molecular cancer,* 24, 150.

MORALEVA, A., ANTIPOVA, N., PAVLOV, P., DOBROCHAEVA, K. & RUBTSOV, Y. 2026. Nucleolus as a cornerstone linking proliferation and metabolism to cellular responses to stress: involvement of transcription factors MYC and p53. *Frontiers in Molecular Biosciences,* 13, 1749992.

RASSAMEGEVANON, T. 2020. *Translation and optimization of a gamma H2AX foci assay for the prediction of intrinsic radiation sensitivity*. Dissertation, Dresden, Technische Universität Dresden, 2020.

RIZZOTTO, D., ENGLMAIER, L. & VILLUNGER, A. 2021. At a crossroads to cancer: how p53-induced cell fate decisions secure genome integrity. *International journal of molecular sciences,* 22, 10883.

SAKLANI, S. 2024. Recent patterns of cancer incidence and mortality: global and Indian scenario. *Nanoparticles in Cancer Theranostics*, 40-52.